Estimating surface water loss using water deficit indices data and value-added indexes

Guido Masiello[a], Pamela Pasquariello[a], Carmine Serio[a], Vito Telesca[a], Giuliano Liuzzi[a], Marco D'Emilio[a], Rocco Giosa[a], Sara Venafra[b], Italia De Feis[c], Fabio Della Rocca[c,d]

[a]School of Engineering, University of Basilicata, Potenza, Italy
[b]ASI, Rome, Italy
[c]IAC-CNR, Naples, Italy
[d]University of Naples "Federico II", Naples, Italy

Outline

1. Methodology

- ✗ **Water Deficit Index (WDI) & Emissivity Contrast Index (ECI)**

2. Application

- ✗ **Po Valley 2020 and 2022**
- ✗ **Southern Italy during 2015-2023**
- ✗ **Forest site in Northern Italy**
- ✗ **Comparison with WDI and ECI from IASI soundings**

3. Conclusions

Emissivity Contrast Index (ECI)

TIR surface emissivity ($\boldsymbol{\varepsilon}$) is sensitive to soil water content.

Emissivity Contrast:

$$\delta\varepsilon = Max(Channel\ Emissivity) - Min(Channel\ Emissivity);$$

Emissivity Contrast Index (ECI):

$$\mathrm{ECI} = 1 - \delta\varepsilon$$

The closest ECI is to 1, the higher to water content.

Green vegetation (black body)

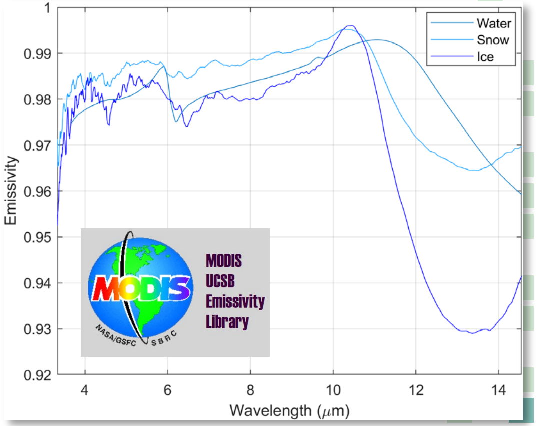

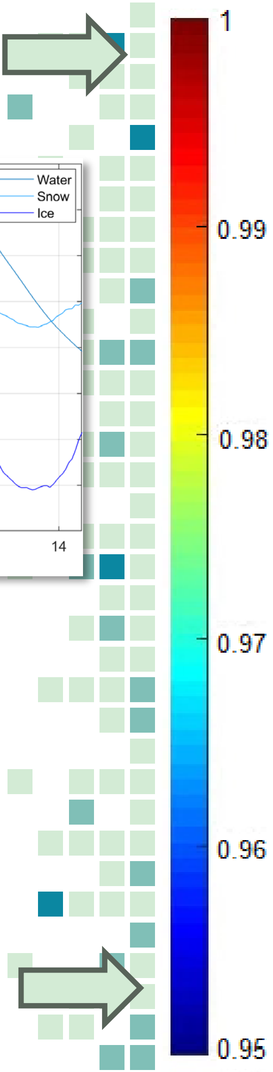

Barren soil

ECI estimation

Emissivity was retrieved from the IASI spectrum using the bands specified in the table below.

Highlight: channel **4.5-5.0 µm** shows a nice contrast between arid soil and green vegetation.

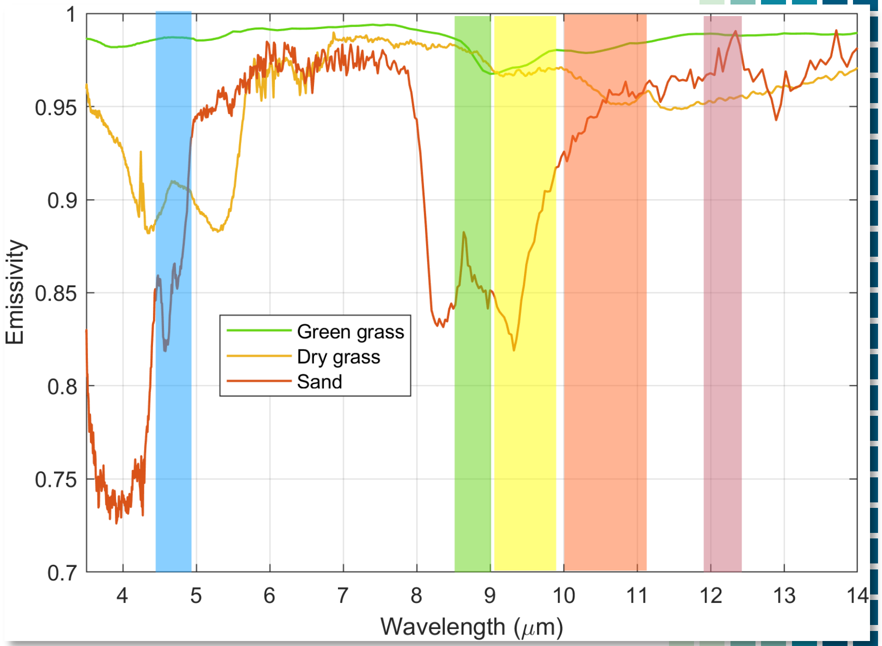

SELECTED BANDS					
λ(µm)	4.5-5.0	8.3-9.1	9.1-10	10-11.1	12-12.5
σ(cm^{-1})	2000-2200	1100-1200	1000-1100	900-1000	800-830
	High brown grass/arid soil contrast.	Reststrahlen band of quartz.	Soil/grass contrast.	Green vegetation	Vegetation

Water Deficit Index (**WDI**)

Dew point temperature (T_d) close to the surface is directly related to evapotranspiration processes.

T_d is obtained combining $\boldsymbol{p}(z_0)$, $\boldsymbol{Q}(z_0)$, $\boldsymbol{T}(z_0)$.

$T_s - T_d$ is related to water loss from surface and vegetation to the atmosphere: the higher the difference, the faster the water loss.

$$WDI = T_s - T_d$$

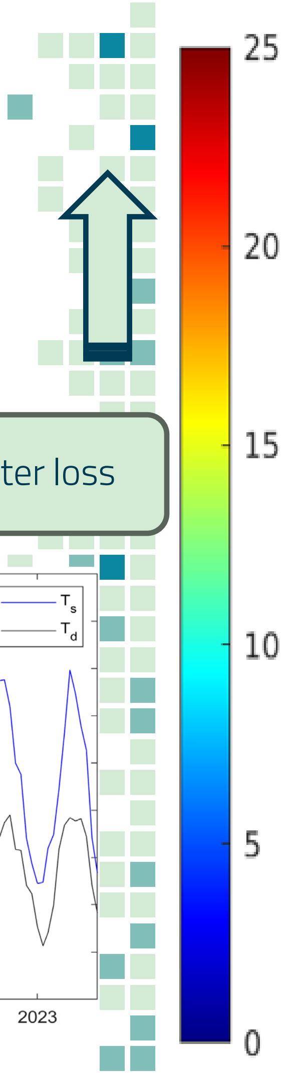

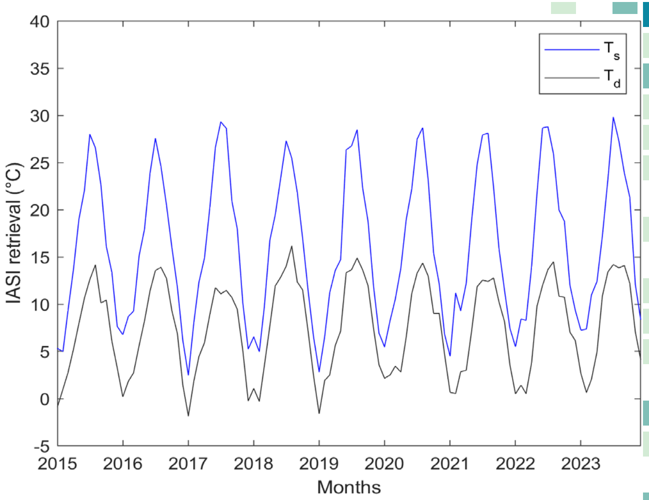

Retrieval methodology

Applied Spectroscopy

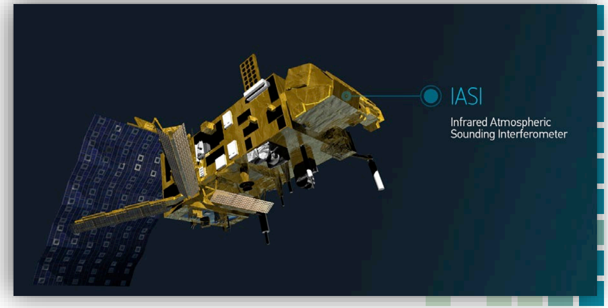

IASI radiances

ECMWF background

Colocation & Preprocessing

MATLAB

Φ-IASI

Inverse

Direct

δ -IASI

σ -IASI

$$\boldsymbol{V} = (T_S, \boldsymbol{T}, \boldsymbol{Q}, \boldsymbol{O}, \boldsymbol{HDO}, \boldsymbol{q_{CO2}}, \boldsymbol{q_{OCS}}, f_{N2O}, f_{CO}, f_{CH4}, f_{SO2}, f_{HNO3}, f_{NH3}, f_{CF4}, \boldsymbol{\varepsilon})$$

Monitoring surface water stress using hyperspectral infrared satellite observations

Φ-IASI REFERENCES

Journal of Quantitative Spectroscopy & Radiative Transfer 312 (2024) 108814

Contents lists available at ScienceDirect

Journal of Quantitative Spectroscopy and Radiative Transfer

journal homepage: www.elsevier.com/locate/jqsrt

The new σ-IASI code for all sky radiative transfer calculations in the spectral range 10 to 2760 cm^{-1}: σ-IASI/F2N

Guido Masiello [a,*], Carmine Serio [a], Tiziano Maestri [b], Michele Martinazzo [b], Fabrizio Masin [b], Giuliano Liuzzi [a], Sara Venafra [c]

[a] Scuola di Ingegneria, Università della Basilicata, Potenza, Italy
[b] Dipartimento di Fisica e Astronomia, Università di Bologna, Bologna, Italy
[c] Agenzia Spaziale Italiana, ASI, Roma, Italy

Journal of Quantitative Spectroscopy & Radiative Transfer 329 (2024) 109211

Contents lists available at ScienceDirect

Journal of Quantitative Spectroscopy and Radiative Transfer

journal homepage: www.elsevier.com/locate/jqsrt

Demonstration of a physical inversion scheme for all-sky, day-night IASI observations and application to the analysis of the onset of the Antarctica ozone hole: Assessment of retrievals and consistency of forward modeling

Carmine Serio [a,*], Guido Masiello [a], Giuliano Liuzzi [a], Angela Cersosimo [a], Tiziano Maestri [b], Michele Martinazzo [b], Fabrizio Masin [b], Giorgia Proietti Pellicia [b], Sara Venafra [c], Claude Camy-Peyret [d]

[a] Scuola di Ingegneria, Università della Basilicata, Potenza, Italy
[b] DIFA, Università di Bologna, Bologna, Italy
[c] Agenzia Spaziale Italiana, ASI, Roma, Italy
[d] Institut Pierre-Simon Laplace, IPSL, Paris, France

MDPI remote sensing

Physical Retrieval of Land Surface Emissivity Spectra from Hyper-Spectral Infrared Observations and Validation with In Situ Measurements

by Guido Masiello [1,*], Carmine Serio [1], Sara Venafra [1], Giuliano Liuzzi [2], Laurent Poutier [3] and Frank-M. Göttsche [4]

land MDPI

Article

The IASI Water Deficit Index to Monitor Vegetation Stress and Early Drying in Summer Heatwaves: An Application to Southern Italy

Guido Masiello [1,*], Francesco Ripullone [2], Italia De Feis [3], Angelo Rita [4], Luigi Saulino [4], Pamela Pasquariello [1], Angela Cersosimo [1], Sara Venafra [1,*] and Carmine Serio [1]

1 Scuola di Ingegneria, Università della Basilicata, 85100 Potenza, Italy
2 Scuola di Scienze Agrarie, Forestali, Alimentari ed Ambientali, Università della Basilicata, 85100 Potenza, Italy
3 Istituto per le Applicazioni del Calcolo "Mauro Picone", IAC-CNR, 80131 Napoli, Italy
4 Dipartimento di Agraria, Università di Napoli Federico II, 80055 Portici, Italy
* Correspondence: guido.masiello@unibas.it (G.M.); sara.venafra@unibas.it (S.V.)

Applied Spectroscopy

Using ECI & WDI together

ECI

The lower the ECI, the lower the water content.

+

WDI

The higher the WDI, the higher the water loss

Confirmation of water loss happening when the indices show an opposite trend over the selected area.

From L2 to L3

IASI-retrieved parameters on a non-evenly-distributed grid (level 2).

Remapping and upscaling (level 3).

Monthly maps are produced.

Processing level	Resolution
L2	12 km
L3	5 km

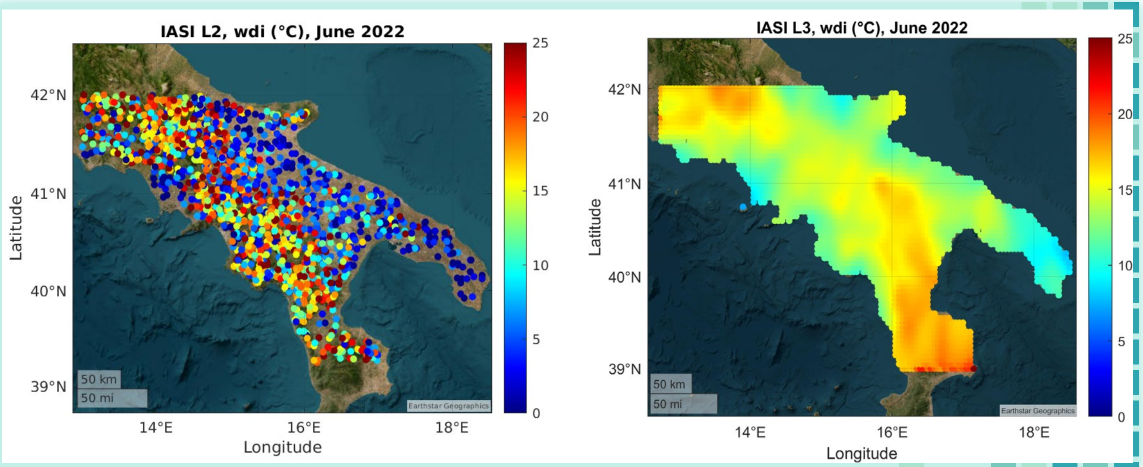

Po Valley Drought

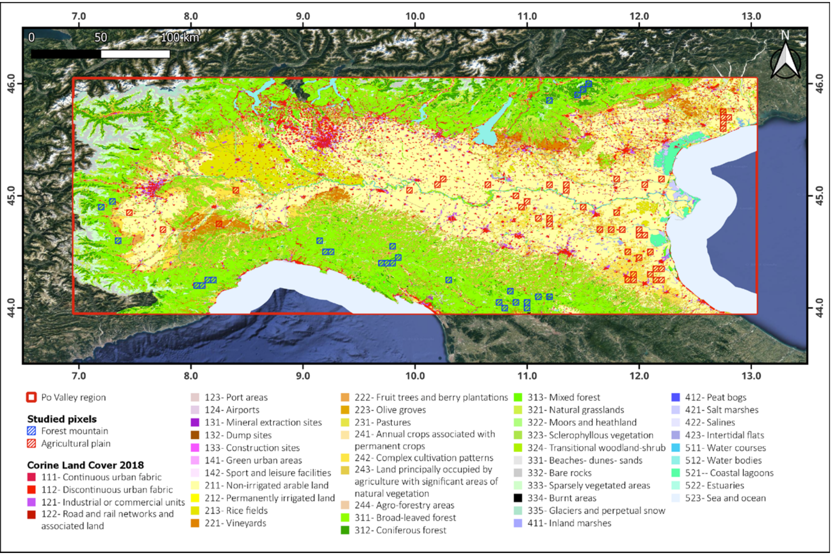

During 2022, the Po Valley region, driven by the incredible snowfall deficit over the Italian Alps (with an average snowfall deficit of 45% for the year), Was affected by an unprecedented hydrological drought with a –85% Po River discharge in July near the river delta

WDI Po Valley, 2022

comparing month by month we notice that in 2022 the wdi values were always higher by up to 10° compared to the values observed for 2020.
Della Rocca et al. (2023) http://doi.org/10.1117/12.2679718

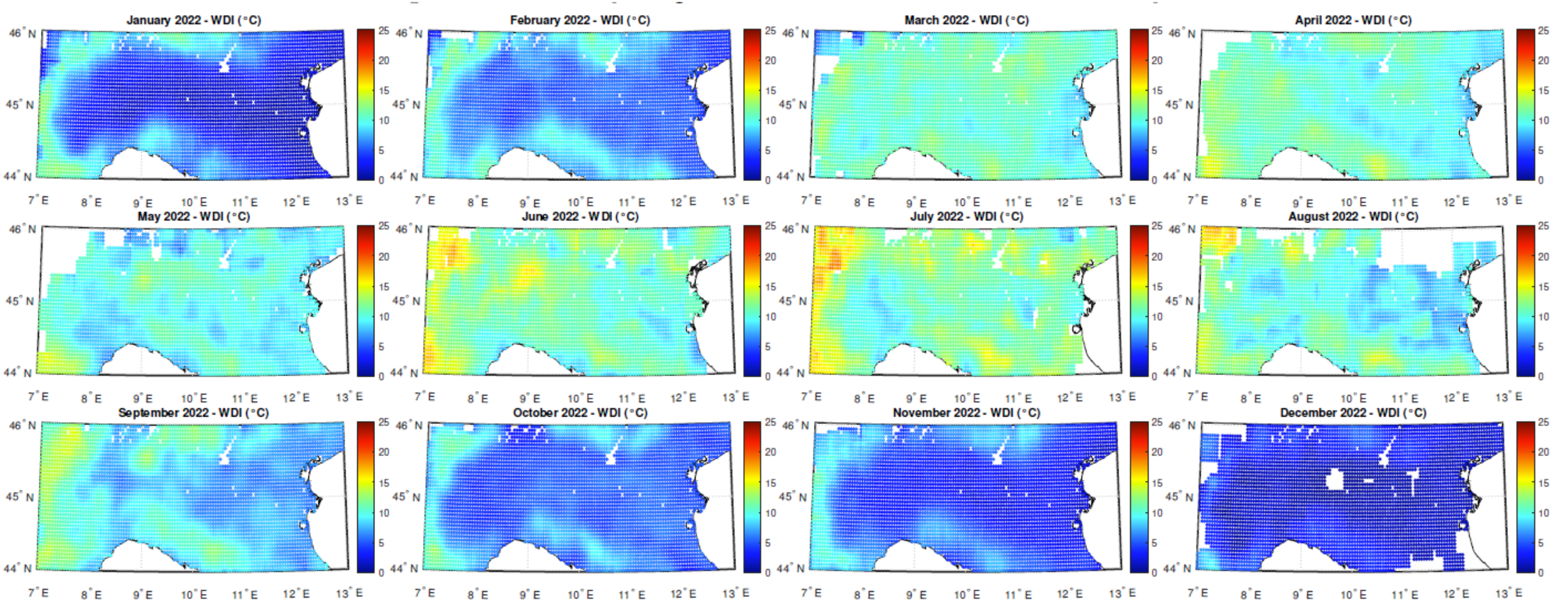

WDI, Po Valley, 2020

comparing month by month we notice that in 2022 the wdi values were always higher by up to 10° compared to the values observed for 2020.
Della Rocca et al. (2023) http://doi.org/10.1117/12.2679718

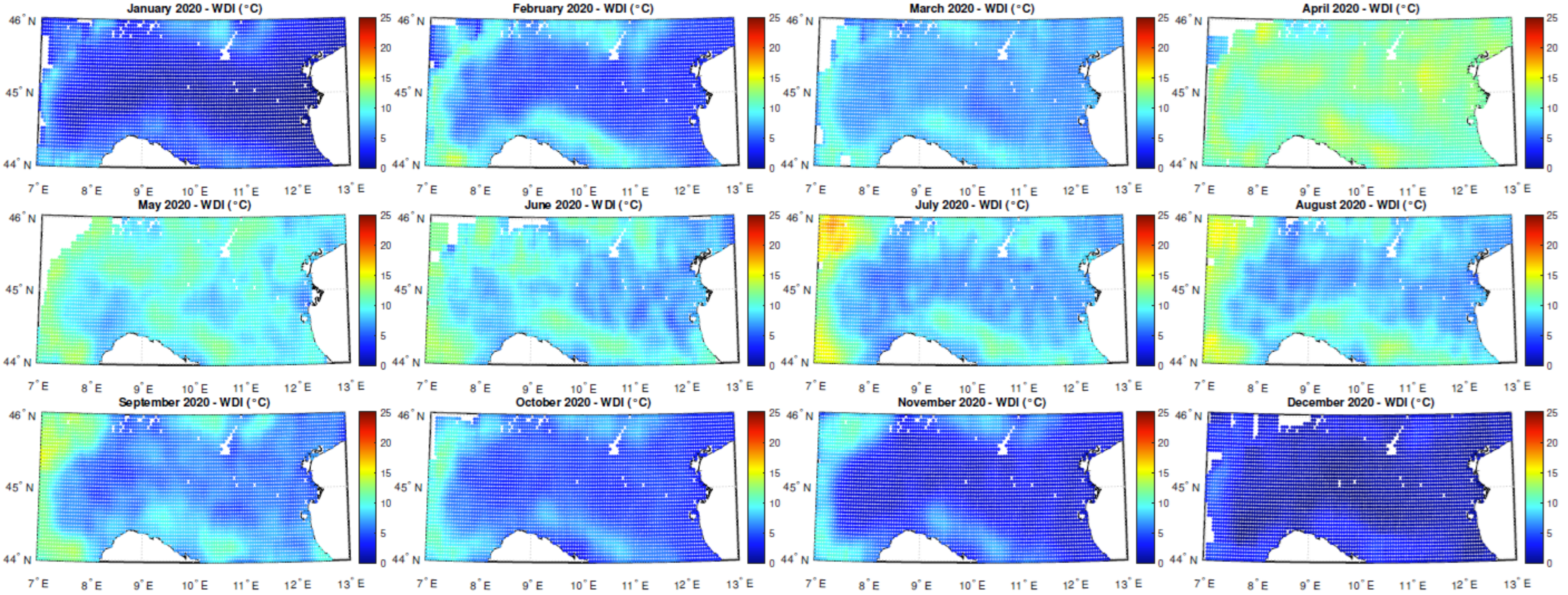

Ground stations

Station alias	Location name	Lat, Lon	Altitude (m.a.s.l)	Variables	Acquisition interval	Provided by
G	Genzano di Lucania	40.79°, 16.00°	315	Air temperature, relative humidity	1 hour	ALSIA
P	Pierfaone	40.50°, 15.76°	1473	Air temperature, relative humidity	1 hour	Protezione Civile

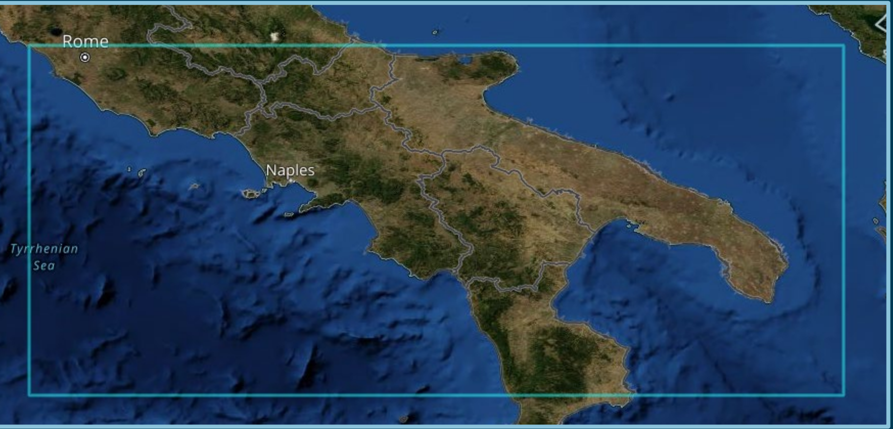

Genzano di Lucania (**Station G**)

Pierfaone (**Station P**)

ECI (2023)

ECI is higher over the coast, while it shows lower values over the forested, inland regions. It also decreases during summer where cultivated fields are located (distinguishes between bare soils and dry vegetation).

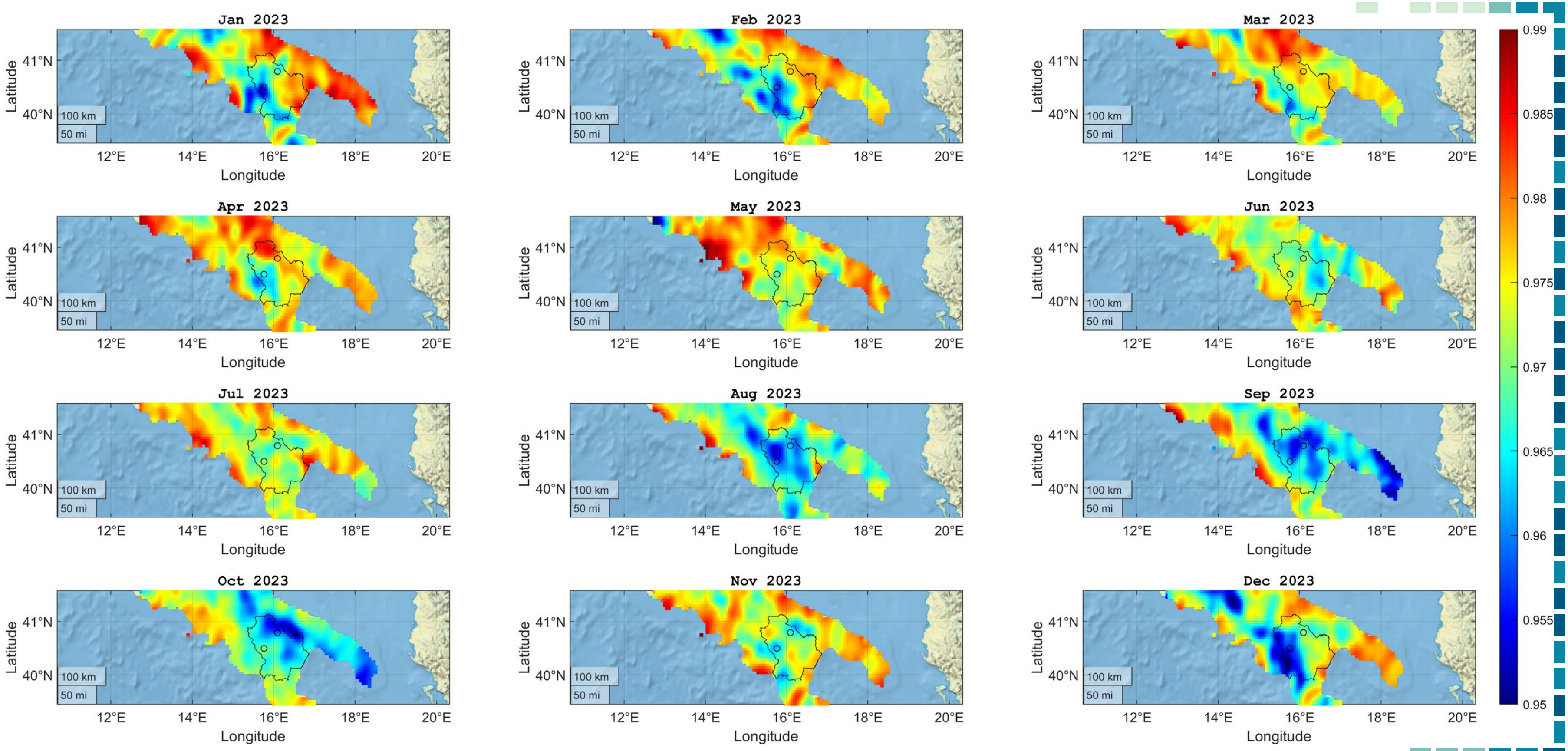

WDI (2023)

WDI values rise during summer on the Apennines forests (≈20 °C difference from January to August), showing an opposing trend with respect to ECI.

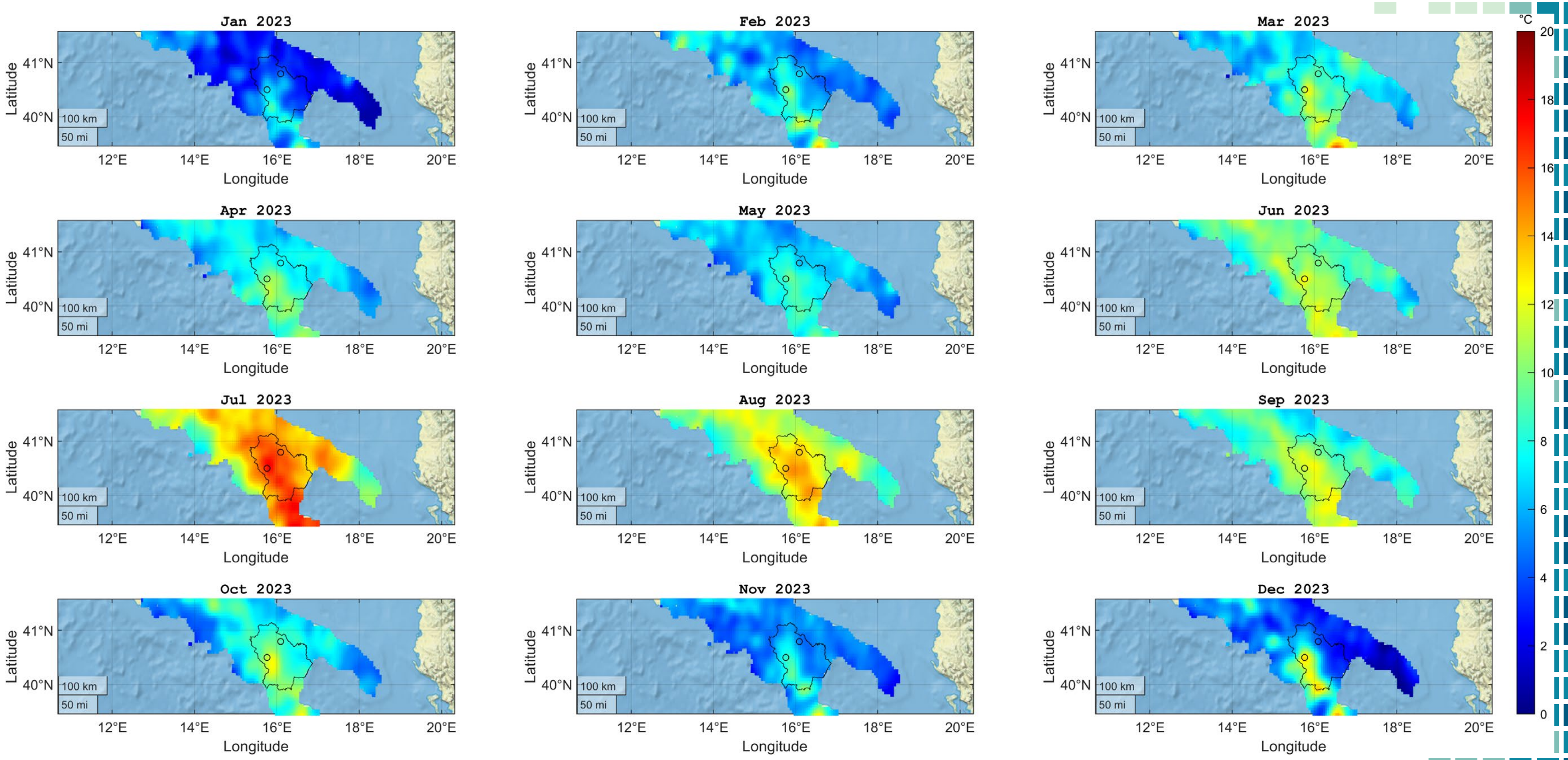

WDI (2015-23) – Genzano di L. (field)

The mean error remains below 1 °C for the cultivated field.

The two T_d curves closely overlap, with their differences peaking at values between 1 and 2 °C only during the summers of 2019 and 2021.

High consistency between the WDI measured at station G and the corresponding satellite retrieval for the same area.

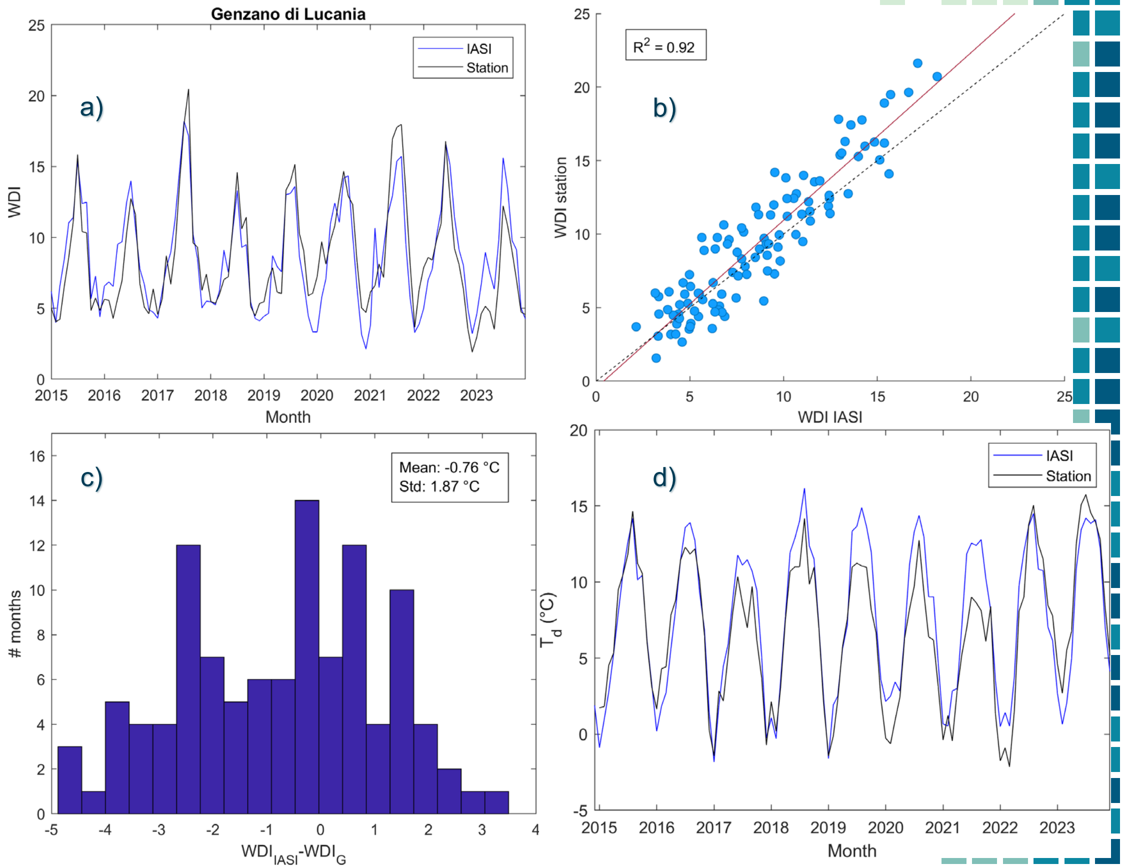

WDI (2015-23) – Pierfaone (forest)

The mean error increases to 3.07 °C for the selected forest.

IASI-retrieved and measured T_d show more stability during summer, while during each winter season in-situ T_d drops to negative values as low as −10 °C and IASI T_d tends to 0.

This discrepancy is probably related to the differences between the broader area covered by the large IASI IFOV and the specific location of the station itself.

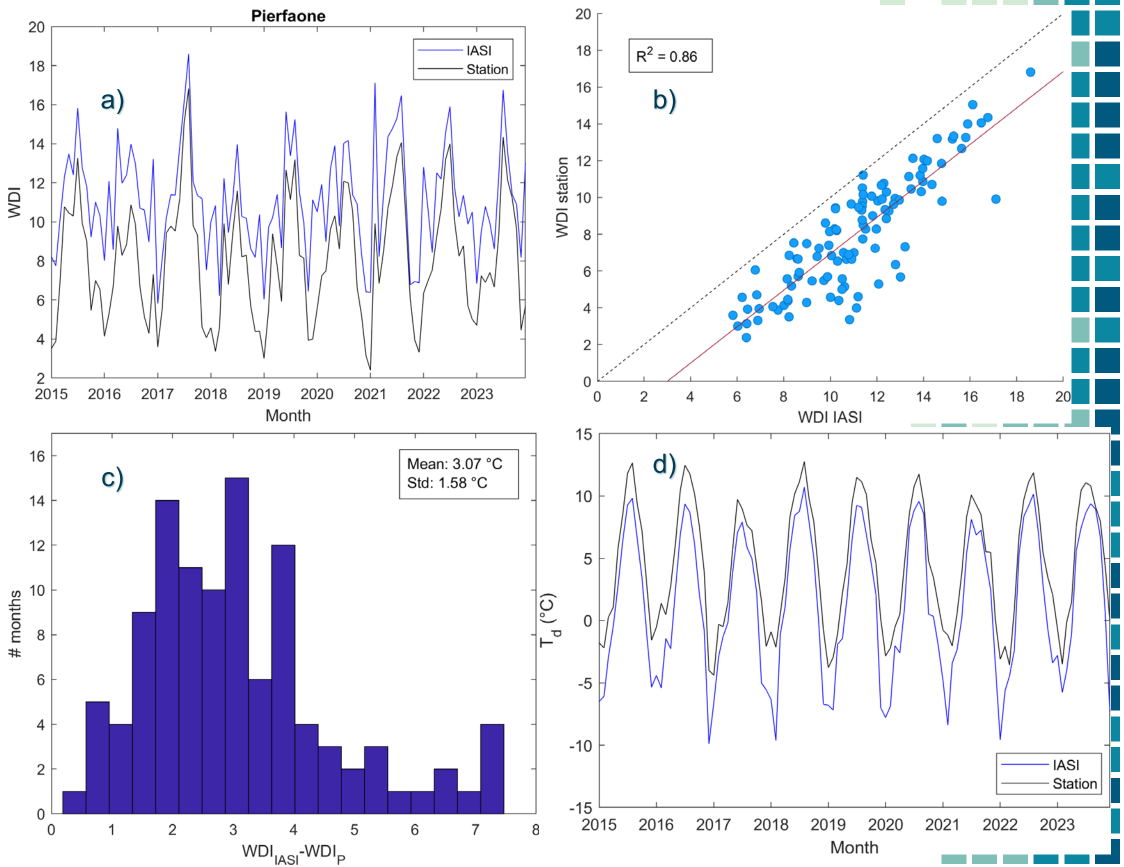

ECI&WDI (2015-23)

ECI and WDI exhibit an inverse relationship over the cultivated field, especially during the summer months, whereas over the woodland, they generally show a positive correlation with occasional divergent behavior, particularly during the summers of 2017 and 2023.

This suggests a more consistent water stress pattern for the cultivated land and a more sporadic one for the woodland.

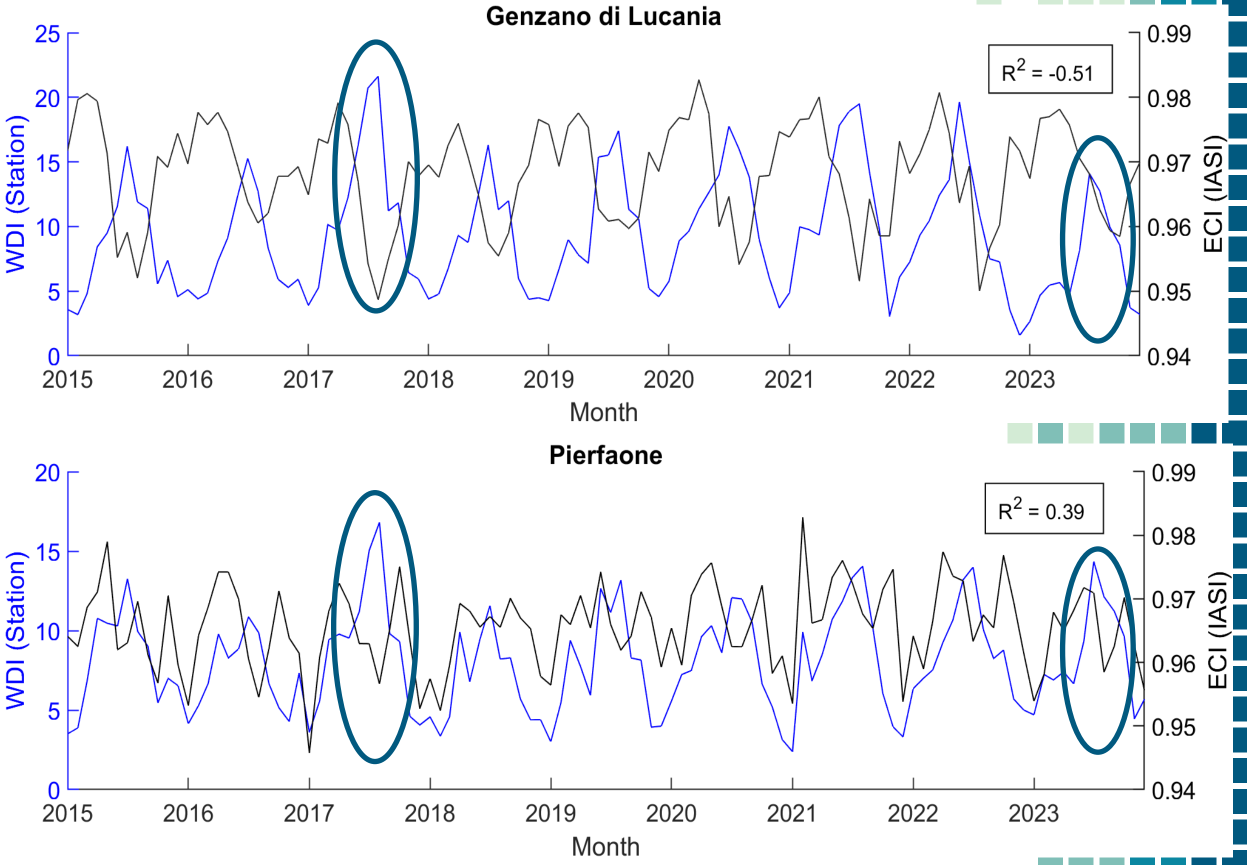

WDI Applications

We also apply these indices to woodlands in northern Italy comparing with Evapotranspiration (ET) from ground-based measurements using ECMWF analysis for Ts-Td (WDI)
Torresani et al. 2022 https://doi.org/10.3390/land11111903

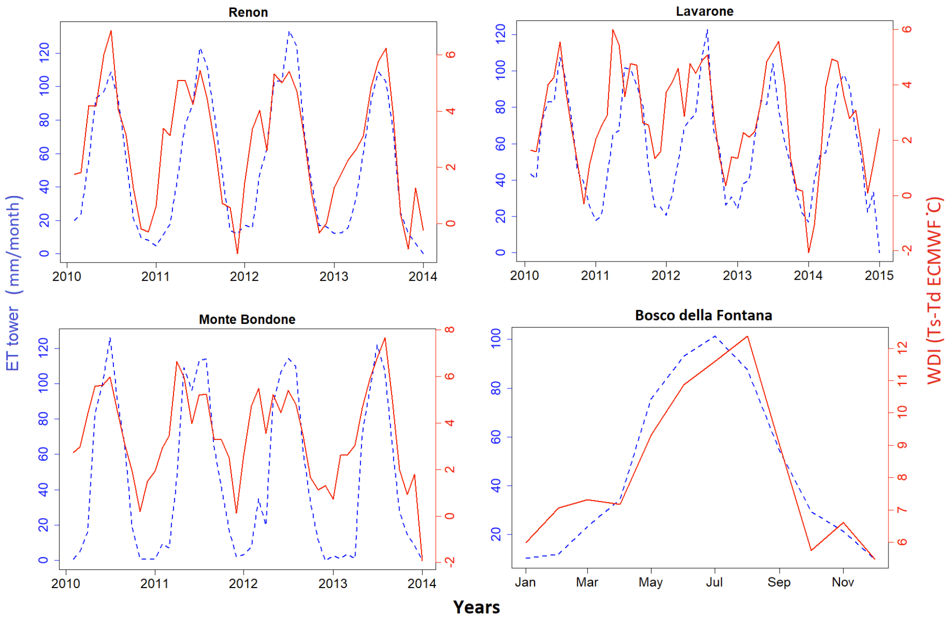

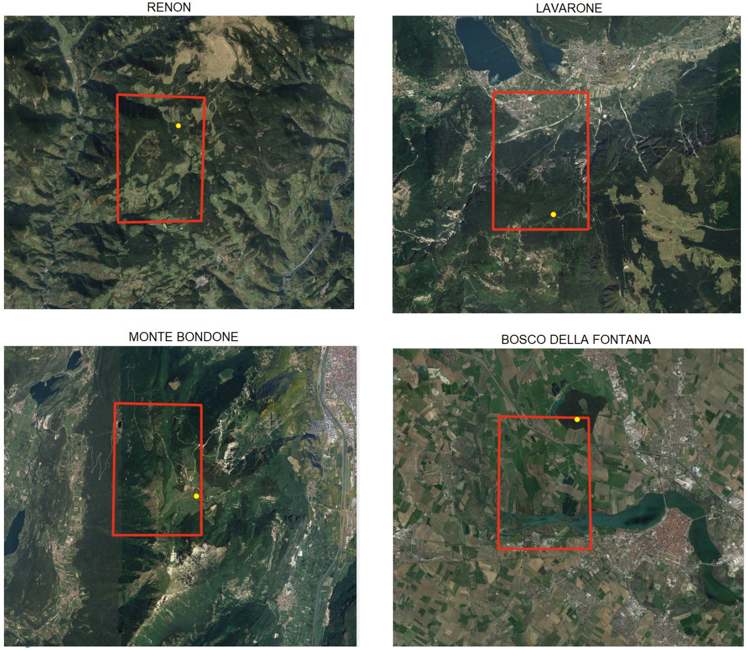

ECI Applications

We also apply these indices to woodlands in northern Italy comparing with Evapotranspiration (ET) from ground-based measurements using CAMEL Emissivity for ECI.

Torresani et al. 2022. https://doi.org/10.3390/land11111903

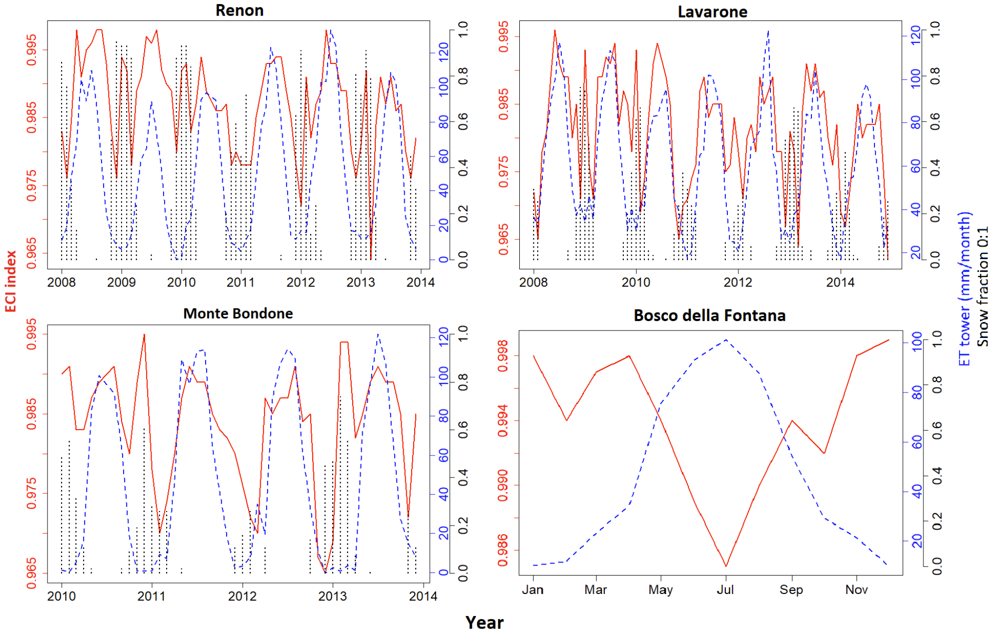

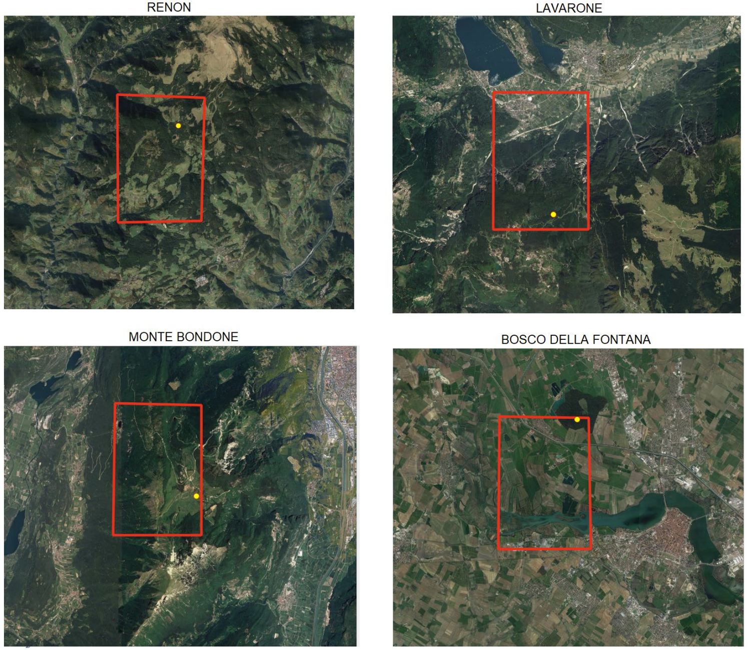

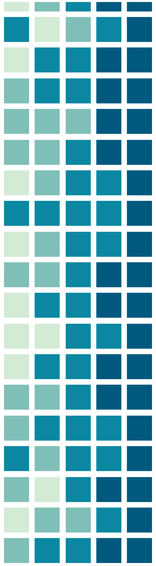

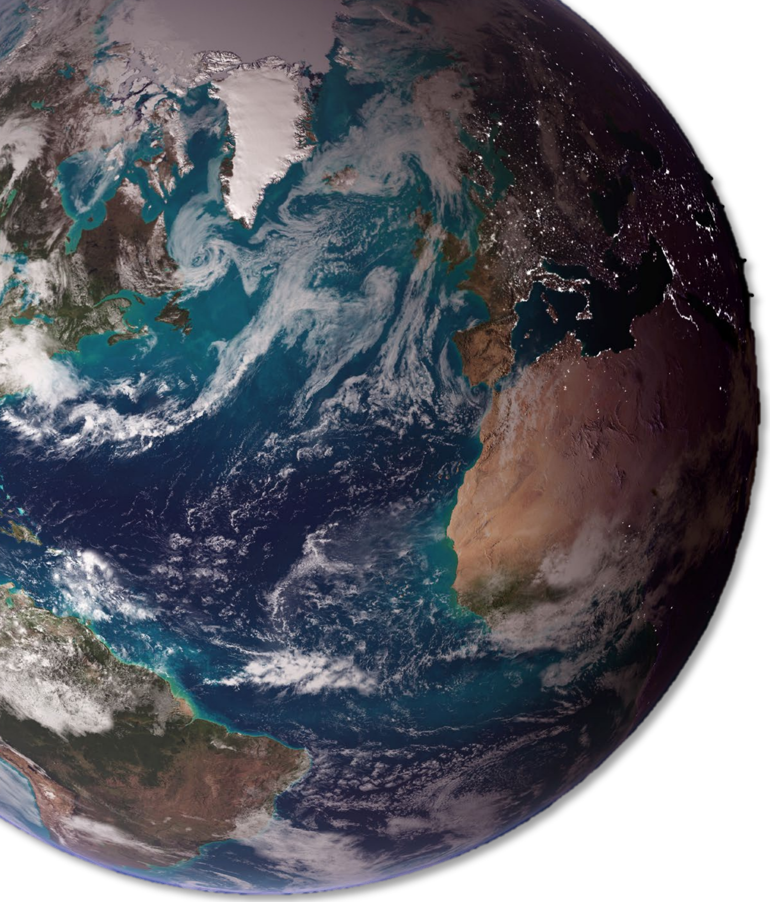

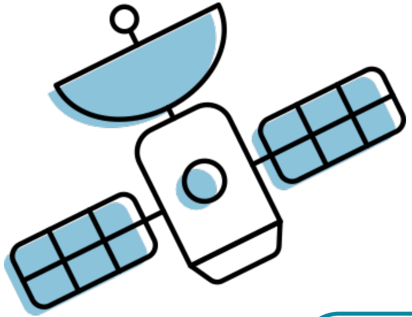

Summing up

- WDI&ECI, estimated from hyperspectral TIR data, as valuable indices to identify surface water stress.
- Interesting correlations between in-situ measurements and satellite observations for WDI considering two different land covers (field and woodland).
- WDI&ECI synergy applicable to both land covers.

Thank you for your attention!

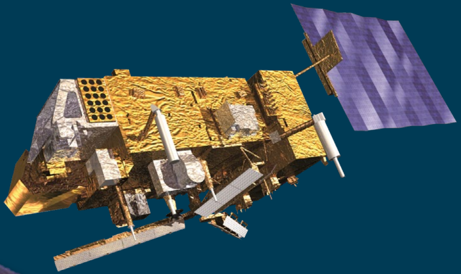

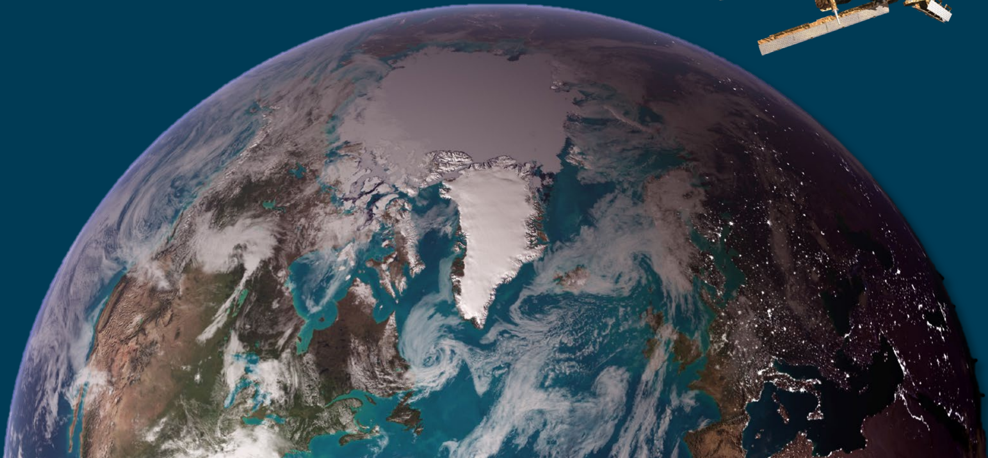

UNIVERSITA DEGLI STUDI DELLA BASILICATA 1982

Applied Spectroscopy

Further developments

- Using the Weather Research and Forecasting (**WRF**) model to further validate the proposed methodology.

- Estimating ECI&WDI from **IASI-N**ew**G**eneration and **FORUM** higher spectral resolution soundings.

- Leveraging **NASA-ASI** SBG-TIR Orbiting Terrestrial Thermal Emission Radiometer (**SBG-OTTER**) to estimate both ECI and WDI at a higher spectral and spatial resolution.

The problem

Water stress in soil and vegetation can be identified using

- In-situ measurements
- Meteorological data
- Remote rensing

Most used indicators: NDVI e air temperature (T_a) close to the surface.

- NDVI from satellite data
- T_a measured in situ or obtained from meteorology

NDVI does not discriminate well between arid soil and senescent vegetation. Moreover, it is not possible to obtain both NDVI and T_a from the same source (spatial and temporal coherence not always guaranteed)

The proposed solution

- Using physical parameters (surface emissivity, surface temperature and dew point temperature) to estimate two new water deficit indices.
- Retrieving them from remote-sensed data acquired by the same instrument, thus ensuring spatial and temporal coherence, and global coverage.

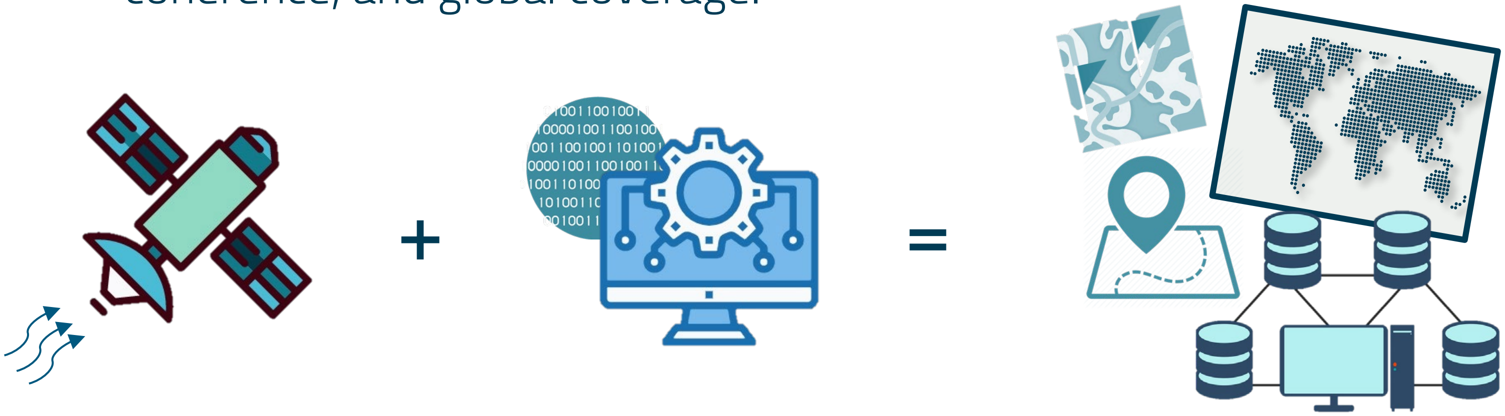

The problem

Climate change, heatwaves and droughts.

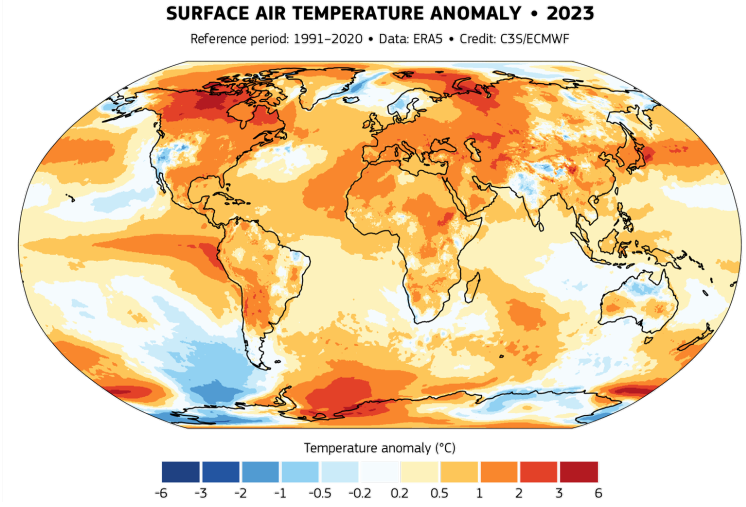

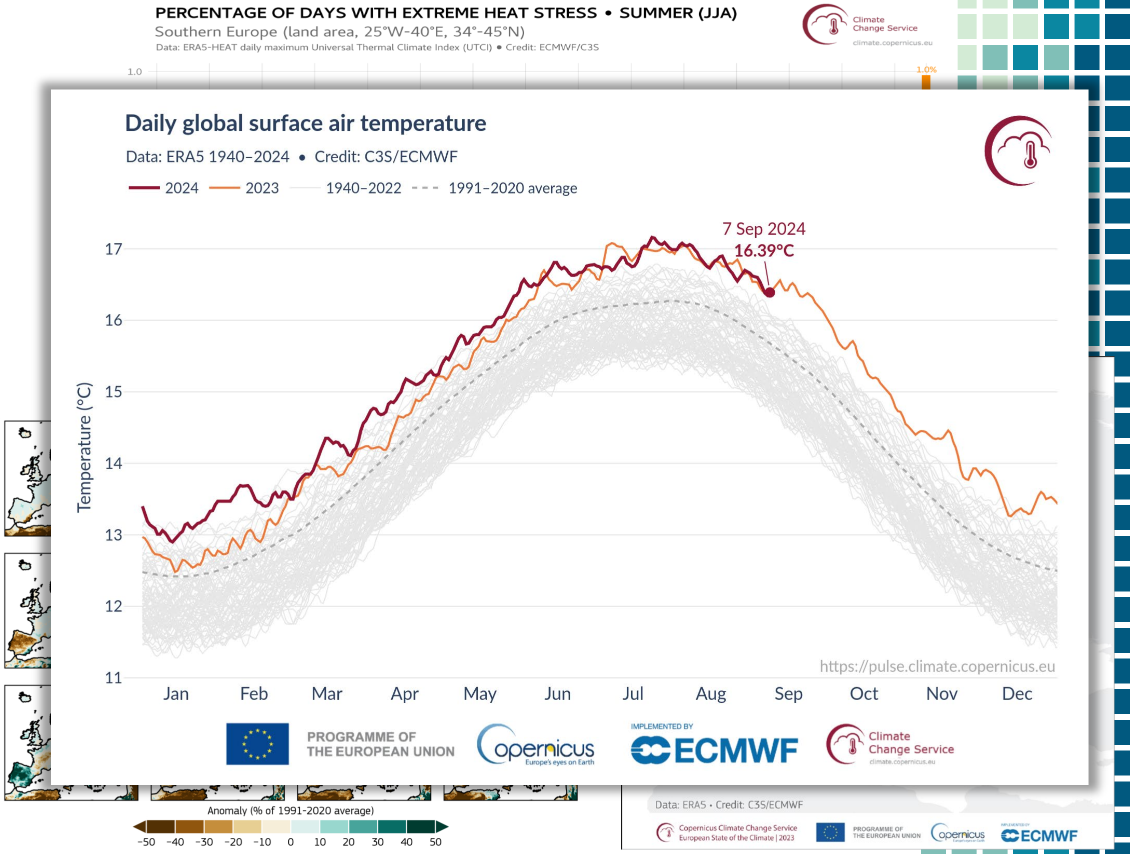

Why Southern Italy?

Droughts & fires have been occurring every summer over the last 10 years

The 2017 drought was one of the most intense, followed by the ones occurred in 2021 and 2023.

The most intense and numerous fire outbreaks of the entire Italian peninsula occur in its southern part.

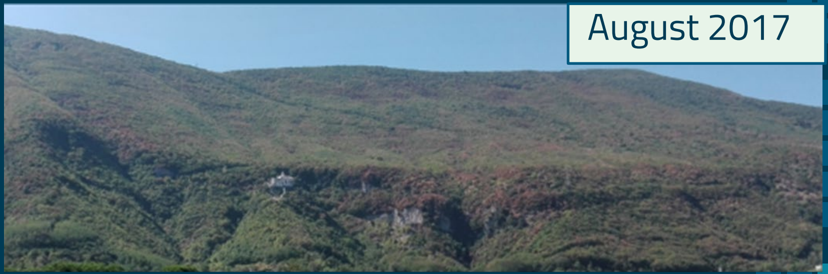

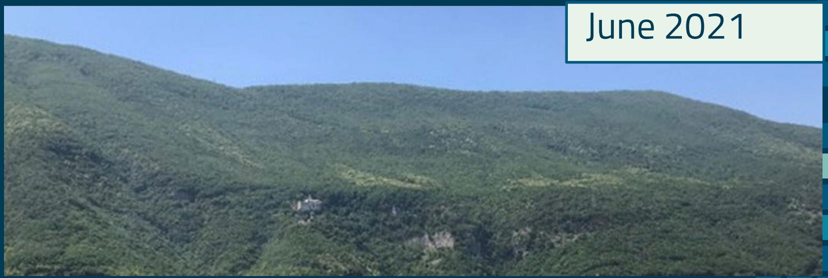

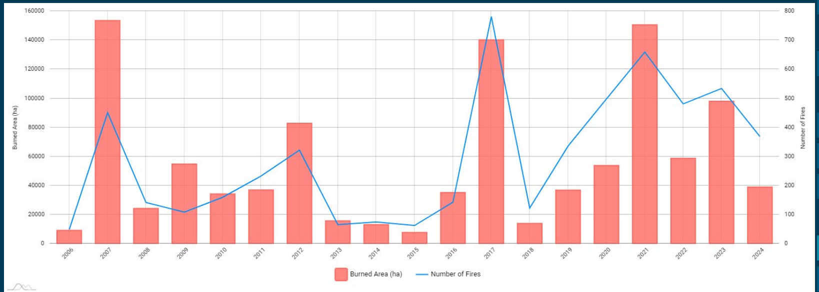

https://effis.jrc.ec.europa.eu/apps/effis.statistics/estimates

MetOp(-A/B/C)

EUMETSAT

Part of EUMETSAT Polar System (EPS)

Orbital period: 101.4 min

Repeat cycle: 29 days (412 orbits)

Global Earth coverage: 2 times per day

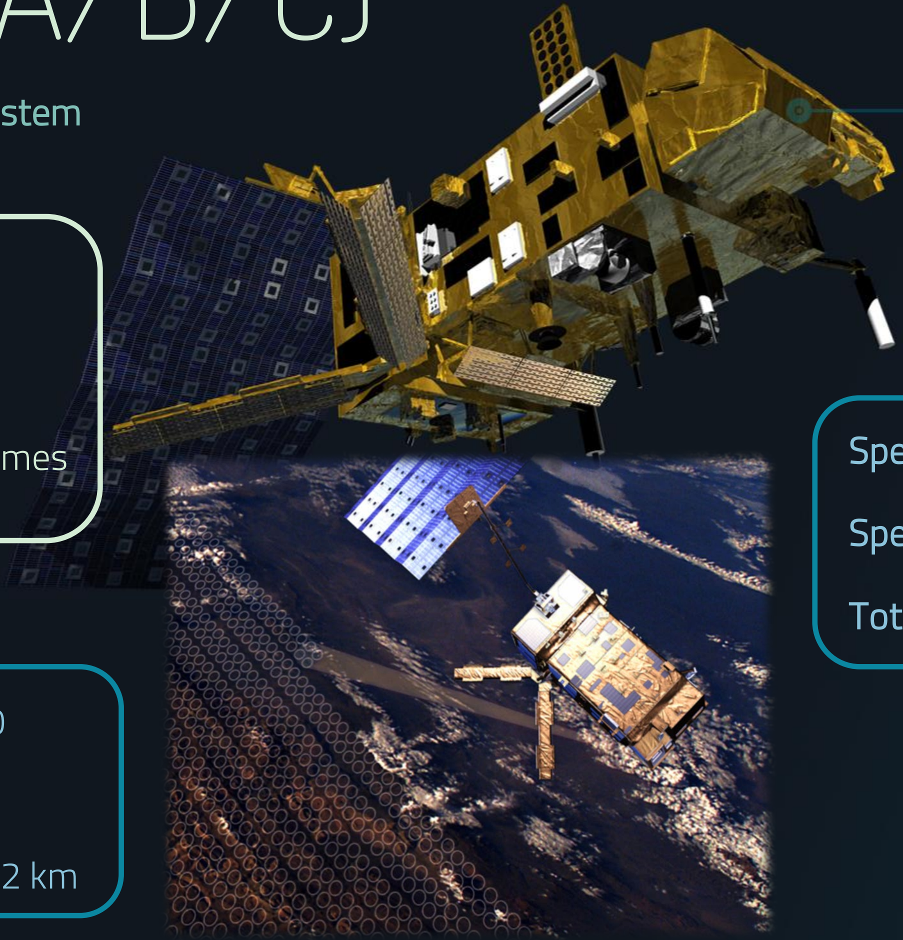

IASI

Infrared Atmospheric Sounding Interferometer

Spectral coverage: 3.4-15.5 µm

Spectral resolution: 0.25 cm-1

Total channels: 8461

FORs per scan: 30

IFOVs per FOR: 4

IFOV resolution: 12 km

Rectangle: SW: 39°, 12° NE: 42°, 19°

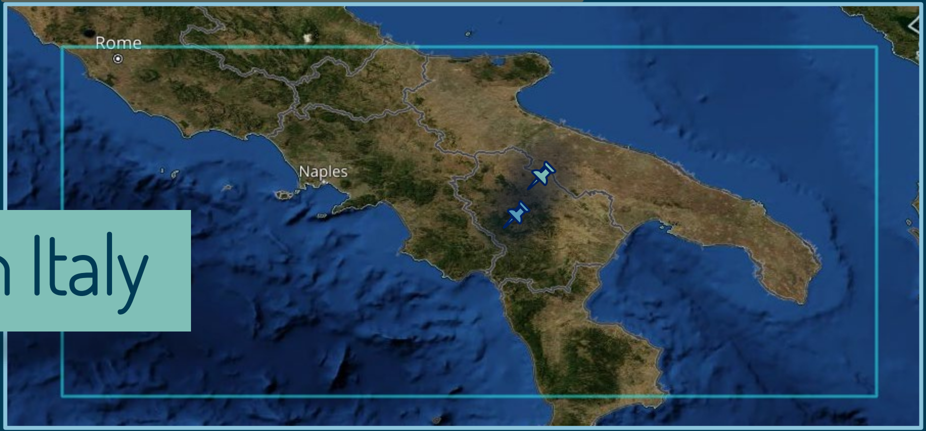

Southern Italy

Basilicata region

2015-2023

Genzano di Lucania (**Station G**)

Pierfaone (**Station P**)

Dew point temperature estimation

- Relationship between partial water vapor pressure p_w and water mixing ratio close to the surface $\boldsymbol{Q}(z_0)$:

$$p_w = \boldsymbol{p}(z_0) \cdot \boldsymbol{Q}(z_0) \cdot R$$

where $R = \frac{m_w}{m_{air}} \cdot 10^{-3}$, m_{air} e m_w air and water molecular mass.

- Relationship between saturation water vapor pressure p_{ws} and air temperature close to the surface $\boldsymbol{T}(z_0)$, relative humidity rh estimation:

$$p_{ws} = 10^{-2} \frac{\exp\left(34.494 - \frac{4924.99}{\boldsymbol{T}(z_0)+237.1}\right)}{(\boldsymbol{T}(z_0) + 105)^{1.57}}$$

$$rh = \frac{p_w}{p_{ws}}$$

- Estimating T_D close to the surface (*Magnus equation*, $-45\ °\mathrm{C} < \boldsymbol{T}(z_0) < 50\ °\mathrm{C}$):

$$T_D = \frac{243.12 \cdot \left[\log(rh) + \frac{243.12 \cdot \boldsymbol{T}(z_0)}{17.62 + \boldsymbol{T}(z_0)}\right]}{17.62 - \left[\log(rh) + \frac{243.12 \cdot \boldsymbol{T}(z_0)}{17.62 + \boldsymbol{T}(z_0)}\right]}$$

From L2 to L3

$$\bar{x} = \left(\sum_{i=1}^{N} \frac{p_i}{\sigma_i^2} \right)^{-1} \sum_{i=1}^{N} \frac{p_i}{\sigma_i^2} \hat{x}_i$$

$$p_i = \exp\left(-\frac{1}{2} \frac{d^2(\bar{x}, \hat{x}_i)}{d_{th}^2} \right)$$

IASI-retrieved parameters on a non-evenly-distributed grid (level 2).

Remapping and upscaling (level 3).

Monthly maps are produced.

Processing level	Resolution
L2	12 km
L3	5 km

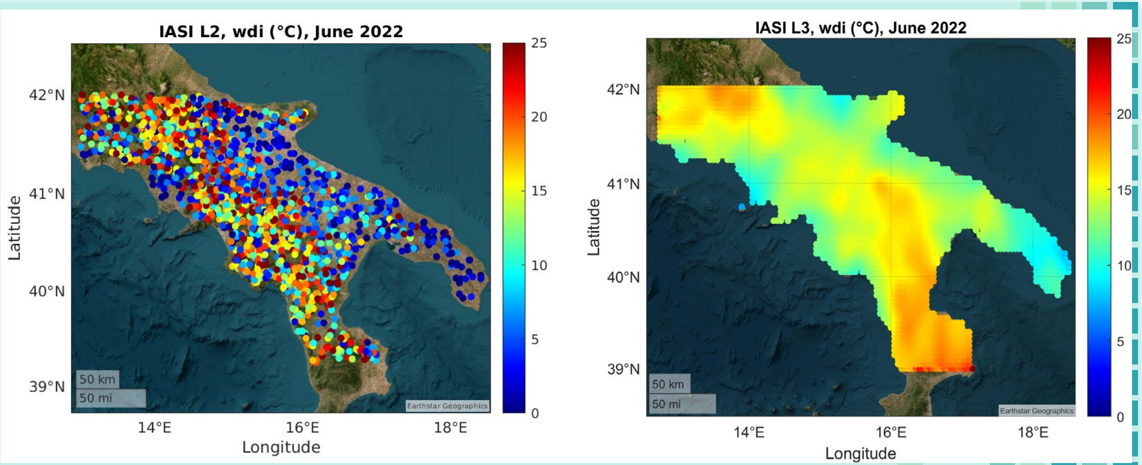

WDI (2015-23) – Side by side comparison

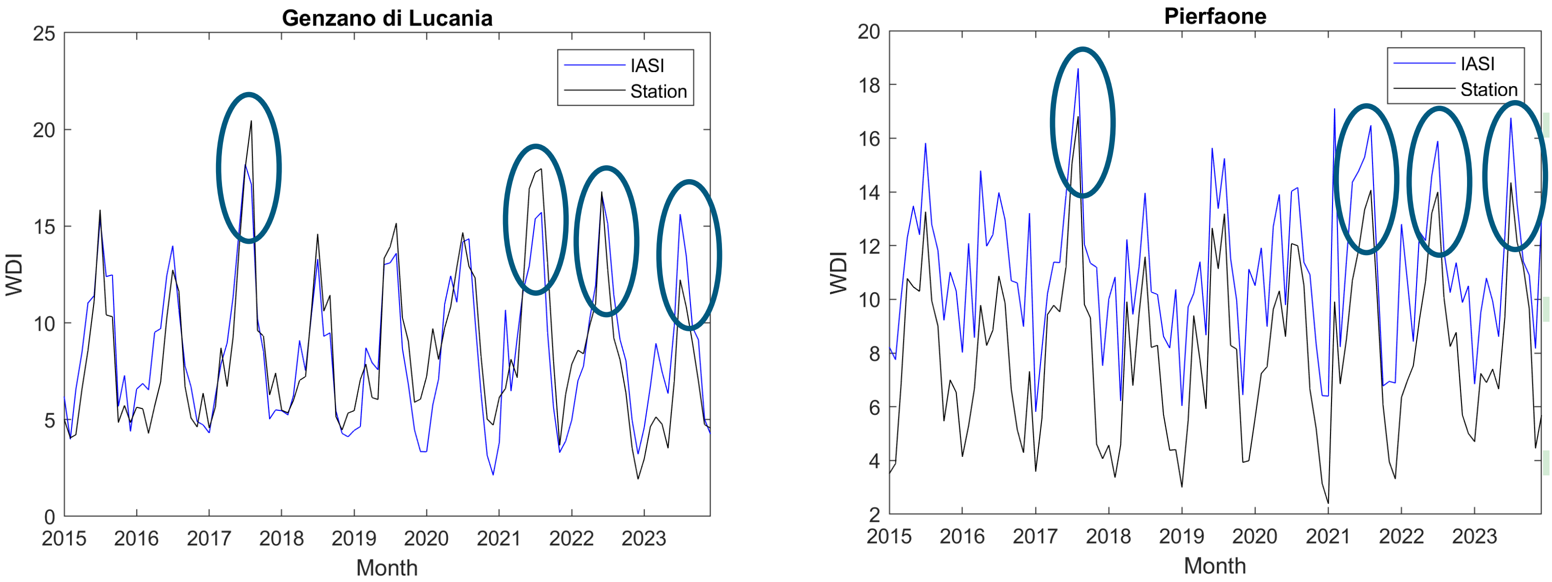

Nonetheless, both WDI estimations effectively highlighted water loss during summer for the two types of land cover. Specifically, the heatwaves of 2017, 2021, 2022, and 2023 were clearly identified in both cases, with peaks of 20 °C for the cultivated field and 14 °C for the forested.